第 32 卷第 10 期
2016 年 10 月

无 机 化 学 学 报
CHINESE JOURNAL OF INORGANIC CHEMISTRY

Vol.32 No.10
1839-1846

原位水解沉积制备高效氮化钽微球太阳能分解水光阳极

杨立恒[1] 罗文俊*[,2,3] 李明雪[4] 邹志刚*[,3]

([1]南京大学现代工程与应用科学学院,南京 210093)

([2]江苏省柔性电子重点实验室,先进材料研究院,江苏先进生物与化学制造协同创新中心,南京工业大学,南京 211816)

([3]南京大学环境材料与再生能源研究中心,固体微结构国家重点实验室,南京大学物理学院,南京 210093)

([4]中国矿业大学物理学院,徐州 221116)

摘要: 利用一种新的原位水解沉积方法, 以在高湿度空气中老化的甲醇中作为溶剂, 通过乙醇钽水解而成前驱体微球颗粒沉积,制备出了高效的 Ta_3N_5 微球光电极,其 1.6 V(vs RHE)电极电位下的光电流值达到了 6.6 mA·cm^{-2}。相反地,在新鲜的甲醇溶液中没有钽前驱体微球颗粒沉积。这表明甲醇中水的含量对 Ta_3N_5 微球光电极的形成十分重要。另外,本制备方法也能方便地在其他透明导电衬底上制备出 Ta_3N_5。

关键词: 太阳能水分解; Ta_3N_5 光阳极; 微球; 原位沉积; 湿度

中图分类号: O614.51+3 **文献标识码**: A **文章编号**: 1001-4861(2016)10-1839-08

DOI: 10.11862/CJIC.2016.330

In Situ Hydrolysis Deposition of an Efficient Ta_3N_5 Microsphere Photoanode for Solar Water Splitting

YANG Li-Heng[1] LUO Wen-Jun*[,2,3] LI Ming-Xue[4] ZOU Zhi-Gang*[,3]

([1]*College of Engineering and Applied Science, Nanjing University, Nanjing* 210093, *China*)

([2]*Key Laboratory of Flexible Electronics & Institute of Advanced Materials, Jiangsu National Synergetic Innovation Center for Advanced Materials, Nanjing Tech University, Nanjing* 211816, *China*)

([3]*Eco-materials and Renewable Energy Research Center (ERERC), National Laboratory of Solid State (Microstructures, Colledge of Physics, Nanjing University, Nanjing* 210093, *China*)

([4]*Department of Physics, China University of Mining and Technology, Xuzhou, Jiangsu* 221116, *China*)

Abstract: A new *in situ* hydrolysis deposition method was used to prepare a Ta_3N_5 microsphere photoanode, which indicates a high photocurrent of 6.6 mA·cm^{-2} at 1.6 V vs RHE. Microsphere precursor films are formed by hydrolysis of $Ta(OEt)_5$ and subsequent deposition on substrates, which is achieved by aging methanol solvent in air with high humidity. In contrast, no precursor films were obtained on substrates with fresh methanol. The results suggest that water in solvent is very essential to *in situ* depositing Ta_3N_5 photoanode. In addition, the facile method can be used to deposit Ta_3N_5 on other transparent conducting substrates.

Keywords: solar water splitting; Ta_3N_5 photoanodes; microsphere; *in situ* deposition; humidity

收稿日期:2016-04-26。收修改稿日期:2016-08-18。

国家重点基础研究发展计划(973 计划, No.2013CB632404, 2014CB239303)、江苏省自然科学基金(No.15KJB150010, BK20140197)、南京大学纳米技术江苏省重点实验室开放研究基金资助项目。

*通信联系人。E-mail:iamwjluo@njtech.edu.cn,zgzou@nju.edu.cn

0 Introduction

Since a TiO_2-based photoelectrochemical (PEC) cell was reported to split water into H_2 and O_2 under illumination, solar water splitting has been considered to be a promising technology to produce H_2 on a large scale[1]. Ta_3N_5 is regarded as one of the most promising candidates due to its high theoretical energy conversion efficiency (15.9%) and suitable band positions [2-3]. Many preparation methods, such as thermal oxidation and nitridation of Ta foil, through-mask anodization, anodization combined with hydrothermal method, electrophoretic deposition, drop-casting and magnetron sputtering, have been reported to prepare Ta_3N_5 [4-9]. However, p-n tandem photoelectrochemical cell requires efficient and translucent/transparent Ta_3N_5 photoanode, which still remains unfulfilled. Therefore, it is still desirable to explore new preparation methods of Ta_3N_5 films. In addition, spherical structure can lead to efficient light absorption and improve performance of a photoelectrode [10-11]. However, current preparation methods for spheres are often in the assistance of additional reagents, which increases preparation cost[12-13].

Herein, an efficient microsphere Ta_3N_5 photoanode was prepared by a new *in situ* hydrolysis deposition method without any additional reagents. Microsphere precursor films were firstly deposited on substrates in tantalum ethoxide ($Ta(OEt)_5$) solution of aged methanol. After oxidation and nitridation, microsphere Ta_3N_5 films were obtained. A 6.6 mA·cm^{-2} photocurrent was achieved at 1.6 V vs RHE. In this context, exploration of new preparation method and the synthesis mechanism of Ta_3N_5 film are our research focus and we hope it can give some hints for preparation of efficient and translucent/transparent Ta_3N_5.

1 Experimental

1.1 Preparation of Ta_3N_5 microsphere photoanodes

A typical preparation procedure of Ta_3N_5 microsphere photoanode is as follows. Firstly, methanol (Purity≥99.5%, Nanjing Chemical Reagent Co., Ltd.) was aged in air with 7% relative humidity at 25 ℃ for 4 h before use. Secondly, 10 mmol·L^{-1} precursor solution of tantalum ethoxide (Purity ≥ 99.95%, Zhuzhou Cemented Carbide Group Corp., Ltd) was prepared with aged methanol. Then, Ta foils (Purity ≥99.95%, Zhongnuo Advanced Material Technology Co., Ltd) were immersed in $Ta(OEt)_5$ methanol solution and films were deposited at 7 ℃ for 48 h. Next, the obtained films were rinsed with deionized water and dried in air at room temperature, followed by calcination in air at 250 ℃ for 30 minutes. Finally, Ta_3N_5 microsphere photoanodes were obtained by nitridation of oxidized samples in a horizontal tube furnace at 850 ℃ for 500 min under 800 mL·min^{-1} NH_3 flow (Referred as Ta_3N_5/aged and Ta_3N_5/aged/Co-Pi for pristine and Co-Pi loaded samples, respectively). In order to investigate the effect of aging methanol, a reference sample was prepared in fresh methanol as solvent under the same conditions (Referred as Ta_3N_5/fresh and Ta_3N_5/fresh/Co-Pi for pristine and Co-Pi loaded samples, respectively).

1.2 Photo-assisted electrodeposition of Co-Pi co-catalyst

Following previous studies, Co-Pi co-catalyst was electrodeposited on Ta_3N_5 film by chronopotentiometry under illumination with constant current of 50 μA for 4 min [5]. The electrodeposition was conducted in a three-electrode cell, with the solution of 0.5 mmol·L^{-1} $Co(NO_3)_2·6H_2O$ (Purity≥99.0%, Shanghai Zhenxin Reagent Factory) and 0.1 mol·L^{-1} $K_2HPO_4·3H_2O$ (Purity≥99.0%, Shanghai Lingfeng Chemical Reagent Co., Ltd.) buffer at pH=7 as electrolyte. Ta_3N_5 was used as working electrode, Pt foil as counter electrode and saturated calomel electrode (SCE) as reference electrode. An AM 1.5G-simulated sunlight simulator (Oriel 92251A-1000, light intensity=100 mW·cm^{-2}) was used as light source. During the deposition process, Co^{2+} was oxidized into Co^{3+} [14-15]. The total amount of charge was about 20 mC·cm^{-2}. Assuming that Faradaic efficiency was 100%, the amount of deposited Co was calculated as follow:

$$N_{Co} = 20\times10^{-3}/96\ 485 = 0.2\ (\mu mol\cdot cm^{-2}) \quad (1)$$

Where N_{Co} is the amount of Co-Pi deposited on Ta_3N_5 per square centimeter. 96 485 ($C \cdot mol^{-1}$) is the Faradaic constant.

After Co-Pi deposition, the electrode was rinsed with deionized water and dried in air for use.

1.3 Characterization of samples

The crystal structures of samples were determined by an X-ray diffractometer (XRD, Rigaku Ultima Ⅲ) with Cu $K\alpha$ ray (λ=0.154 3 nm) at 40 kV and 40 mA. The range is from 10° to 80°. Morphologies of electrodes were observed on a field emission scanning electron microscope (SEM, Zeiss, Ultra 55-44-08) at an accelerating voltage of 15 kV. Water content of methanol was measured on a moisture analyzer (Metrohm, KF787 Titrino). Absorption spectra were investigated on a UV-vis spectrophotometer (Shimadzu, UV-2550). FTIR spectra were obtained on a Nexus870 spectrophotometer in the range of 4 000 ~400 cm^{-1}. Thermogravimetric analysis was carried out in air with a Netzsch STA 449F3 instrument by increasing temperature from 30 to 600 ℃ with 5 ℃·min^{-1}.

1.4 Photoelectrochemical measurements

Photoelectrochemical performance was measured in a three-electrode cell using an electrochemical analyzer (CHI-633C, Shanghai Chenhua). Ta_3N_5 microsphere electrode was used as working electrode, Pt foil as counter electrode and saturated calomel electrode (SCE) as reference electrode. Aqueous solution of 1 mol·L^{-1} NaOH was employed as electrolyte. A commercial AM 1.5G-simulated sunlight simulator (Oriel 92251A-1000, light intensity =100 mW·cm^{-2}) was used as light source. Current-potential curves were recorded at a scan rate of 10 mV·s^{-1}. The potential of working electrode versus SCE was converted into RHE (reversible hydrogen electrode) potential scale according to the following formula:

$$V_{RHE} = V_{SCE} + 0.242 + 0.059pH \quad (2)$$

where V_{RHE} is the potential versus RHE(V), V_{SCE} is the potential versus SCE (V), and pH is the pH value of electrolyte. The incident photon-to-current efficiency (IPCE) was determined under the irradiation of different wavelength light generated by monochromatic filters according to the following formula:

$$IPCE = 1\,240\, I_{ph} / (P\lambda) \quad (3)$$

where I_{ph} is the photocurrent density ($\mu A \cdot cm^{-2}$), P and λ are the incident light intensity ($\mu W \cdot cm^{-2}$) and wavelength (nm), respectively. The incident light intensity was measured by a photometer (Newport, 84 0-C, USA).

2 Results and discussion

Fig.1 shows photographs of $Ta(OEt)_5$ solution of fresh and aged methanol before and after deposition, respectively. Both solutions are transparent at the beginning. After depositing at 7 ℃ for 48 h, solution of aged methanol became white (Fig.1(b)). However, solution of fresh methanol was still transparent. White films were deposited on substrates in solution of aged methanol, whereas there were no samples on substrates in solution of fresh methanol. The results suggest that film deposition comes from hydrolysis of $Ta(OEt)_5$ in aged methanol. Since the only difference between the two kinds of methanol was the methanol whether exposed in moist air or not, little water in methanol was essential for the formation of films. The water content was measured about 0.15% (w/w) by a moisture analyzer. The detail effect of water will be

Fig.1　Photographs of precursor solution of (a) fresh and (b) aged methanol before and after deposition

discussed below.

XRD patterns were measured to determine phases and crystal structures of the two samples, as shown in Fig.2. Orthorhombic phase Ta_3N_5 (PDF No. 19-1291) was obtained for Ta_3N_5/aged. In contrast, Ta_3N_5/fresh shows no peaks of Ta_3N_5. Fig.3 shows scanning electron microscopy (SEM) images of Ta_3N_5/fresh and Ta_3N_5/aged. Surface and cross-sectional SEM images in Fig.3 (a, c) indicate that Ta_3N_5/fresh shows only morphology of Ta substrate and no Ta_3N_5 is observed. The result is in agreement with the XRD data. However, Fig.3 (b) shows that Ta_3N_5/aged is composed of spherical particles, with the diameter around 1μm. Discernible roughness, many nanopores and cracks are observed on the surface, which come from volume shrinkage from transition of Ta_2O_5 into Ta_3N_5 and the decomposition of residual organics (Fig.4) during nitridation [12]. High magnification SEM image of precursor is displayed in the inset picture of Fig.3 (b). The result suggests that microspheres are formed during precipitation. Fig.3 (d) is the cross-sectional image of Ta_3N_5/aged. It shows that Ta_3N_5 film electrode is composed of microsphere particles and the thickness is about 7.5 μm. From the inset in Fig.3 (d), Ta_3N_5 microsphere is solid and composed of smaller particles, which suggests that Ta_3N_5 microsphere originates from the agglomeration of nanoparticles.

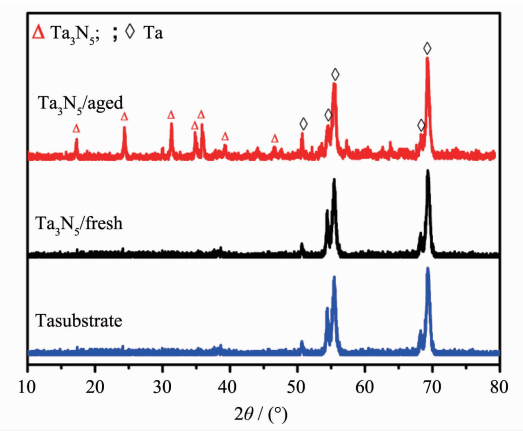

Fig.2 XRD patterns of Ta_3N_5/fresh and Ta_3N_5/aged

Spherical structure is one of favorable microstructures in both photoelectrochemical and solar cells[10-11]. Usually, spherical Ta_3N_5 particles obtained by solution methods are assisted with additional agents [12-13]. Though the distribution size of Ta_3N_5 spheres can be narrowed, introduction of additional reagents actually increases the possibility of inclusion of impurities, as well as experimental difficulties and preparation cost. In our study, however, Ta_3N_5 microsphere was prepared in a more simple way, without any additional agents, and thus those shortcomings are avoided.

FTIR spectra were used to investigate formation process of microsphere, and the results are shown in Fig.4. Peaks below 1 000 cm^{-1} are attributed to stretching, bending and torsion modes of Ta-O [16-17].

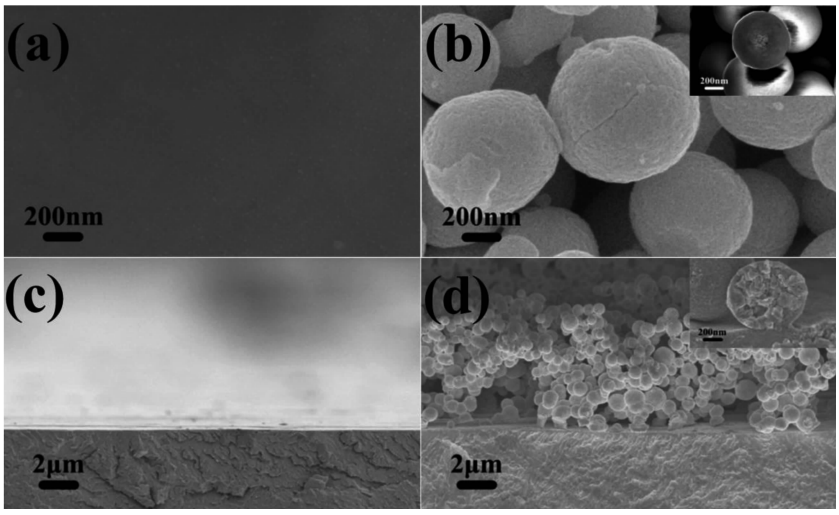

Inset images in (b) and (d) are microsphere precursor and cross-sectional image of cracked Ta_3N_5, respectively

Fig.3 High magnification SEM images of Ta_3N_5/fresh(a) and Ta_3N_5/aged(b); Cross-sectional images of Ta_3N_5/fresh(d) and Ta_3N_5/aged(d)

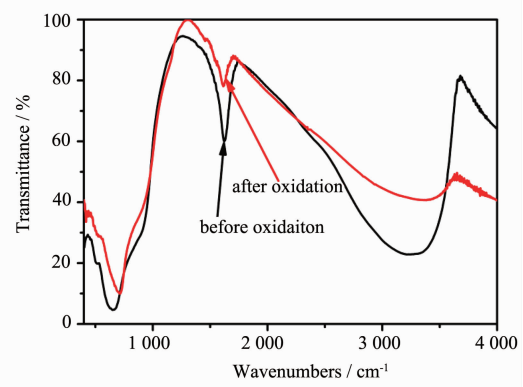

Fig.4　FTIR spectra of microsphere precursor before and after calcined at 250 ℃ for 30 min in air

The broad absorption between 800 and 1 000 cm^{-1} corresponds to the presence of Ta suboxides[18]. A peak at ~3 342 cm^{-1} is assigned to OH stretching modes, and peak at ~1 626 cm^{-1} is associated with OH bending modes[17,19]. Both of them are weakened after calcination at 250 ℃. The existence of -OH group confirms that microsphere is from the hydrolysis of tantalum ethoxide.

In order to further investigate composition of as-deposited microsphere precursor before calcination, thermogravimetric (TG) is measured and the result is shown in Fig.5. The endothermic peak under 100 ℃ comes from evaporation of adsorbed water. Weight loss with exothermic peak ended at around 500 ℃ arises from the decomposition of organics in microsphere, which comes from the organic group $-CH_2CH_3$ of Ta $(OEt)_5$ [16-17]. However, organic compounds cannot be removed completely when calcined at 250 ℃ and thus lead to the formation of Ta suboxides.

According to the above discussion, formation process of Ta_3N_5 microsphere can be concluded as follows with the simplified chemical reactions[20-21]:

Hydrolysis:

$Ta(OR)_5+H_2O \rightarrow$

$Ta(OR)_4(OH)+ROH(R=-CH_2CH_3)$

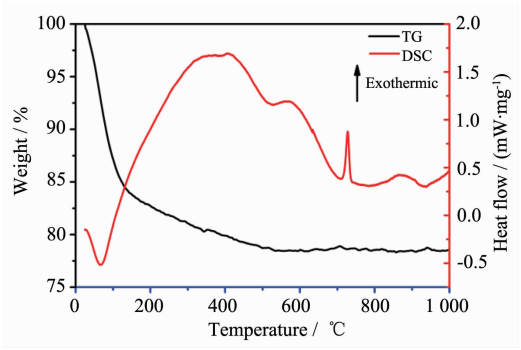

Fig.5　Thermogravimetric spectrum of microsphere precursor

Polycondensation:

$(RO)_4$-Ta-O-H + $Ta(OR)_5 \rightarrow$

$(RO)_4$-Ta-O-Ta-$(OR)_4$+ROH (R=-CH_2CH_3)

Water content in methanol is a key factor to trigger the whole reaction. Actually, the two reactions proceed simultaneously once the hydrolysis-condensation reaction is triggered. As long as a critical radius is reached, nucleation will take place. And nanocrystalline will agglomerate into spherical particle due to its lowest surface energy. Finally, when the spherical particles are big enough, sedimentation happens and a film is deposited on the substrate. After oxidation and nitridation, Ta_3N_5 microsphere film is obtained. A schematic diagram of formation process of Ta_3N_5 microsphere is illustrated in Fig.6.

Fig.7 indicates UV-Vis absorption spectrum of Ta_3N_5 microsphere photoanode. The Ta_3N_5 microsphere film shows a high absorption, which comes from light scattering of microspheres. Contribution from substrate is excluded through the absorption spectrum of Ta_3N_5/fresh. Ambiguous ERERC can be identified through the Ta_3N_5 microsphere film on quartz substrate in the inset(Ⅱ) of Fig.7, which suggests that *in situ* hydrolysis deposition method can be used to prepare a translucent Ta_3N_5 microsphere electrode.

Photoelectrochemical properties of Ta_3N_5 micro-

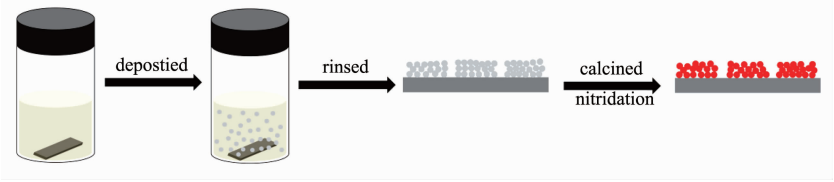

Fig.6　Schematic illustration of formation process of Ta_3N_5 microsphere film

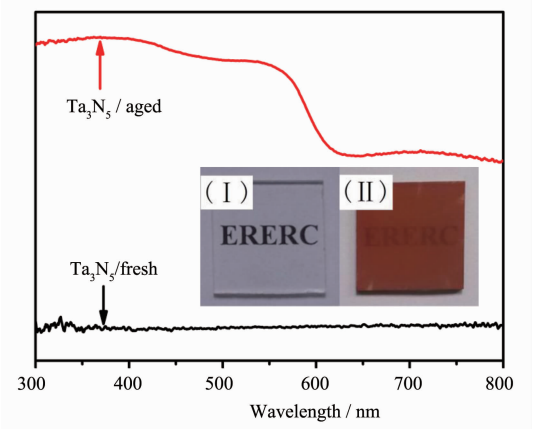

Inset pictures are photographs through (Ⅰ) quartz substrate and (Ⅱ) Ta_3N_5/aged on the quartz substrate, respectively

Fig.7 Absorption spectra of Ta_3N_5/fresh and Ta_3N_5/aged on the quartz substrate

sphere photonodes were measured and the results are shown in Fig.8. In order to exclude contribution of Ta substrate on photocurrent, Ta_3N_5/fresh was also measured as a reference. Dark currents of both electrodes are negligible. The photocurrent of Ta_3N_5/fresh and Ta_3N_5/fresh/Co-Pi is much lower than that of a Ta_3N_5 microsphere photonode. Therefore, photocurrents of Ta_3N_5/aged and Ta_3N_5/aged/Co-Pi entirely come from Ta_3N_5 microsphere, rather than from substrate. Generally, a bare Ta_3N_5 photoanode suffers from severe photo-corrosion in aqueous solution and surface combination, which can be remarkably suspressed by depositing a co-catalyst. Among different co-catalysts, Co-Pi is low-cost and operable under mild conditions [14,22]. Therefore, in this study, Co-Pi (2 μmol·cm^{-2}) was electrodeposited on the Ta_3N_5 film to improve the performance of the Ta_3N_5 microsphere electrode. After deposition of Co-Pi, the photocurrent of Ta_3N_5/aged/Co-Pi is about 3 times as high as that of Ta_3N_5/aged. Current density of Ta_3N_5 microsphere electrode by in situ hydrolysis deposition method is ~2.34 mA·cm^{-2} at 1.23 V vs RHE, and ~6.6 mA·cm^{-2} at 1.6 V vs RHE. A Ta_3N_5 photoanode prepared by EPD indicated 3.18 mA·cm^{-2} photocurrent at 1.23 V vs RHE and about 6 mA·cm^{-2} at 1.6 V vs RHE[23]. High photocurrents of 5.5 mA·cm^{-2} and 6.7 mA·cm^{-2} at 1.23 V vs RHE have been achieved by direct oxidation and nitridation of Ta foil[4-5]. The photocurrent in this study is comparable to samples by EPD and oxidation and nitridation of Ta foil, but much lower than 12.1 mA·cm^{-2} obtained by Ta_3N_5 with integration of hole-storage layer, coupled molecular catalysts and TiO_x blocking layer [6]. However, in this study, preparation conditions and co-catalysts have not yet been optimized. And thus it is promising to further improve Ta_3N_5 microsphere photoanode by in situ hydrolysis deposition method in future work.

Fig.8 (b) is the incident photon-to-current efficiency (IPCE) of Ta_3N_5/fresh/Co-Pi and Ta_3N_5/aged/Co-Pi. The IPCE of Ta_3N_5/fresh/Co-Pi is nearly zero in the spectrum range from 350 to 610 nm, which further excludes contribution of substrate on photocurrent. The IPCE of Ta_3N_5/aged/Co-Pi is ~26% at 400 nm, but decreases at longer wavelength[24]. The integrated

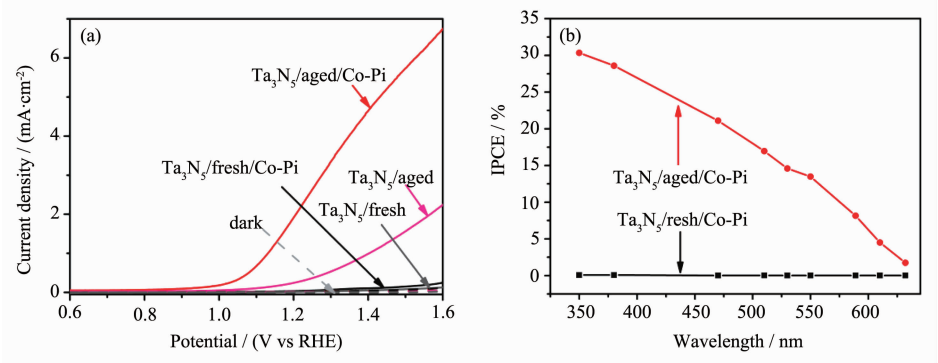

Scan rate: 10 mV·s^{-1}, Electrolyte: 1 mol·L^{-1} NaOH (pH=13.6)

Fig.8 (a) Current-potential curves of Ta_3N_5/fresh, Ta_3N_5/fresh/Co-Pi, Ta_3N_5/aged and Ta_3N_5/aged/Co-Pi in the dark (dash lines) and under AM 1.5G simulated sunlight irradiation (100 mW·cm^{-2}) (solid lines), respectively; (b) IPCE curves of Ta_3N_5/fresh/Co-Pi and Ta_3N_5/aged/Co-Pi at 1.23 V vs RHE

photocurrent (~2.35 mA·cm^{-2}) shown in Fig.9 is very close to the measured value (~2.34 mA·cm^{-2}), which suggests that the measured photocurrent is reliable. The photocurrent response of Ta_3N_5/aged/Co-Pi in IPCE also agrees well with the absorption edge, suggesting that the photocurrent originates from the band gap transition of Ta_3N_5. The stability of Ta_3N_5/aged and Ta_3N_5/aged/Co-Pi was also measured and the result is shown in Fig.10. As we can see, the photocurrent of Ta_3N_5/aged declines over 50% after only 3 ~4 s under illumination, but the time was extended to about 2 000 s for Ta_3N_5/aged/Co-Pi. Though photocurrent of Ta_3N_5/aged/Co-Pi decreases obviously, nonzero photocurrent can still be observed. The stability of Ta_3N_5 microsphere electrode should be further improved in future.

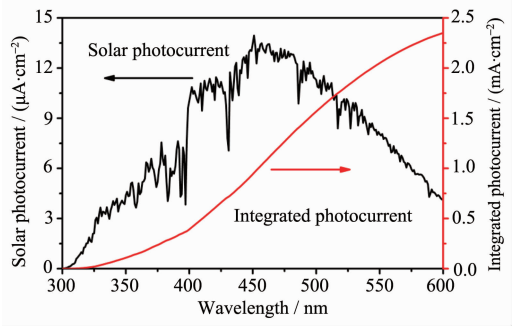

Fig.9　Integrated solar photocurrent at 1.23 V vs RHE from the standard solar spectrum

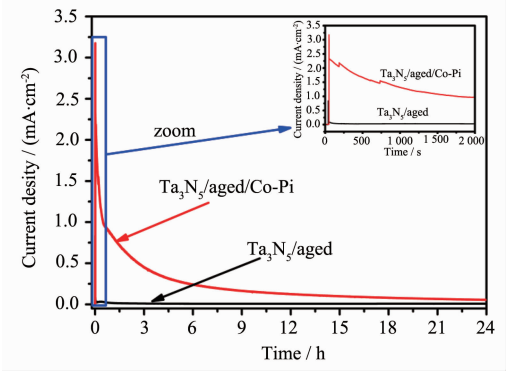

Electrolyte: 1mol·L^{-1} NaOH (pH=13.6)

Fig.10　Current-time curves of Ta_3N_5/aged and Ta_3N_5/aged/Co-Pi measured at 1.23 V vs RHE

3　Conclusions

In summary, we synthesized an efficient Ta_3N_5 microsphere photoanode by a new and facile in situ hydrolysis deposition method. A Ta_3N_5 microsphere film was formed on Ta substrate in $Ta(OEt)_5$ solution of aged methanol. The microsphere is formed by hydrolysis of $Ta(OEt)_5$ and subsequent agglomeration of nanoparticles. Water content in solvent was indispensable to in situ deposition of Ta_3N_5 film. High photocurrent density was obtained on the Ta_3N_5 microsphere electrode, ~2.34 mA·cm^{-2} at 1.23 V vs RHE and ~6.6 mA·cm^{-2} at 1.6 V vs RHE under AM 1.5G simulated sunlight irradiation (100 mW·cm^{-2}). In addition, in situ hydrolysis deposition method is a promising method to prepare efficient Ta_3N_5 photoanodes on other transparent conducting substr ates.

References:

[1] Fujishima A, Honda K. *Nature*, **1972**,**238**:37-38

[2] Wang L, Zhou X, Nguyen N T, et al. *Adv. Mater.*, **2016**,**28** (12):2432-2438

[3] Fu G, Yan S, Yu T, et al. *Appl. Phys. Lett.*, **2015**,**107**(17): 171902

[4] Li M, Luo W, Cao D, et al. *Angew. Chem. Int. Ed.*, **2013**,**52** (42):11016-11020

[5] Li Y, Zhang L, Torres-Pardo A, et al. *Nat. Commun.*, **2013**, **4**:2566

[6] Liu G, Ye S, Yan P, et al. *Energy Environ. Sci.*, **2016**,**9**: 1327-1334

[7] Khan S, Zapata M J M, Pereira M B, et al. *Phys. Chem. Chem. Phys.*, **2015**,**17**:23952-23962

[8] Wang Z, Qi Y, Ding C, et al. *Chem. Sci.*, **2016**,**7**(7):4391-4399

[9] Cong Y, Park H S, Dang H X, et al. *Chem. Mater.*, **2012**,**24** (3):579-586

[10]Pan J H, Wang Q, Bahnemann D W. *Catal. Today*, **2014**, **230**:197-204

[11]Deepak T G, Anjusree G S, Thomas S, et al. *RSC Adv.*, **2014**,**4**(34):17615-17638

[12]Cao J, Ren L, Li N, et al. *Chem. Eur. J.*, **2013**,**19** (38): 12619-12623

[13]Liu X, Zhao L, Domen K, et al. *Mater. Res. Bull.*, **2014**,**49**: 58-65

[14]Kanan M W, Nocera D G. *Science*, **2008**,**321**(5892):1072-1075

[15]Lutterman D A, Surendranath Y, Nocera D G. *J. Am. Chem. Soc.*, **2009**,**131**(11):3838-3839

[16]Ndiege N, Subramanian T W V, Shannon M A, et al. *Chem. Mater.*, **2007**,**19**(13):3155-3161

[17]Zhao D, Jiang H, Gong H, et al. *Transition Met. Chem.*, **2010**,**36**(1):119-123

[18]Fang Q, Zhang J Y, Wang Z, et al. *Thin Solid Films*, **2003**,**428**(1):248-252

[19]Antonelli D M, Ying J Y. *Chem. Mater.*, **1996**,**8**(4):874-881

[20]Sun Y, Sermon P, Vong M. *Thin Solid Films*, **1996**,**278**(1):135-139

[21]Wolf C, Rüssel C. *J. Mater. Sci.*, **1992**,**27**(14):3749-3755

[22]Pramanik M, Li C, Imura M, et al. *Small*, **2016**,**12**(13):1709-1715

[23]Liao M, Feng J, Luo W, et al. *Adv. Funct. Mater.*, **2012**,**22**(14):3066-3074

[24]Hisatomi T, Kubota J, Domen K. *Chem. Soc. Rev.*, **2014**,**43**(22):7520-7535